Copper clusters in mordenite. A direct structural comparison with the NO decomposition catalyst Cu-ZSM-5

Dean C. Sayle,[a] **C. Richard A. Catlow,**[a] **Marc A. Perrin**[b] **and Patrice Nortier**[b]

[a]*Davy-Faraday Laboratory, The Royal Institution of Great Britain, 21 Albemarle Street, London, UK W1X 4BS*
[b]*Centre de Recherche de Rhône-Poulenc, 52 Rue de la Haie Coq, 93308 Aubervilliers Cedex, France*

Using computer simulation techniques we have identified the configuration and location of copper clusters in Cu-mordenite. Fundamental differences are found between these clusters and those generated in an analogous modelling study of Cu-ZSM-5, which, considering the structural similarity between these two zeolitic materials, suggests that the host lattice exerts a critical influence on the configurations of the copper species that form within its internal pore structure. We observe a much reduced occurrence of $Cu^{II}-OH-Cu^{I}$ species, which we suggested previously represents a useful model for the active site in Cu-ZSM-5 and which may therefore provide a structural explanation for the much reduced activity of Cu-mordenite compared with Cu-ZSM-5 for NO decomposition.

Catalysts for the decomposition of NO to form N_2 and O_2, a thermodynamically favourable reaction, are needed for the reduction of air pollution. Various catalysts have been shown to effect this reaction. However, to be of practical interest the activity must be high. The discovery by Iwamoto *et al.*[1] that the Cu-ZSM-5 zeolite can catalyse NO decomposition at high conversion has stimulated much interest in these systems,[2–7] although various problems associated with this system preclude its use commercially.[8] The understanding of the active sites would provide an ideal platform with which to develop improved catalyst systems which do not suffer the inadequacies of the present material.

In a previous study[9] we investigated, at the atomic level, the configurations and location of copper species within the Cu-ZSM-5 system. In particular we proposed models for the active site based on two copper species, bridged by an extra lattice OH group, specifically $Cu^{II}-OH-Cu^{I}$ species.[9] We also note that these species are strongly anchored to the zeolite wall *via* framework aluminium.[10,11] In this work we investigate the configurations of copper species within a mordenite host lattice. We might expect the Cu-mordenite system to exhibit similar activity to the Cu-ZSM-5 system as the host lattices are related,[12] comprising similar interconnecting channel systems and both are based on a 5–1 secondary building unit of silicon TO_4 octahedra (Fig. 1), yet Cu-mordenite exhibits much inferior activity.[13] The results of this study will, by considering a direct structural comparison between the configurations of the copper species within these two systems, help rationalise the origin of this difference in their catalytic behaviour.

Since the primary aim of this study is to examine how the host zeolite actuates the configurations of the copper species that form within its channel system, the Si/Al ratio and copper loading in our model for Cu-mordenite are commensurate with those of our previous study of Cu-ZSM-5 enabling a direct comparison to be made. Any differences between the copper configurations may then be attributed entirely to the influence of the host zeolite. We note however that the Si/Al ratio and copper loading in experimentally observed Cu-mordenite systems of inferior catalytic activity are different from those considered here. However, the differences in the copper cluster structures are likely to be small. Indeed, the procedure used in this study, discussed in greater detail below, for introducing aluminium and extralattice copper species into the host zeolite may result in a particular region of the simulation cell being relatively devoid of aluminium and copper, corresponding to a high Si/Al and low copper loading, resulting, of course, in an alternative region being rich in aluminium and copper due to localised aluminium and copper species. It is therefore expected that the results will provide detailed models for systems with a range of Si/Al and copper loading, including those of the experimentally observed Cu-mordenite. Moreover, it is unlikely that this method will fail to identify any of the significant low energy structures.

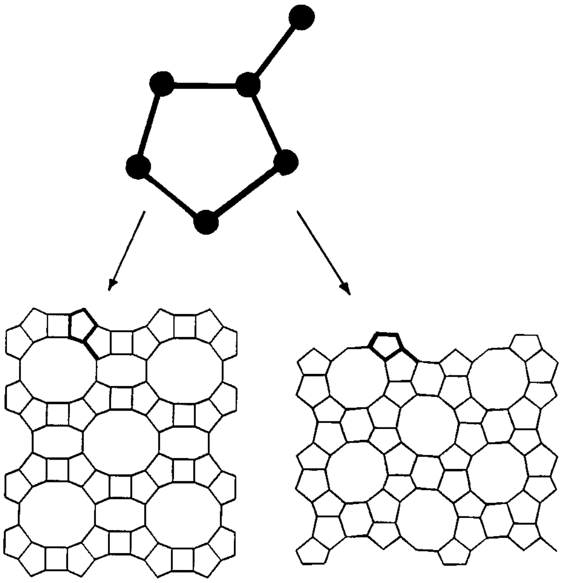

Fig. 1 Representation of the framework structures of mordenite[12] (left) and ZSM-5 (right). The top figure represents the 5–1 secondary building unit on which both zeolites are based. The channel sizes for mordenite and ZSM-5 are: mordenite, [001] 12 ring of size 6.5 × 7.0 Å interconnecting [010] 8 ring of size 2.6 × 5.7 Å; ZSM-5 [100] 10 ring of size 5.1 × 5.5 Å interconnecting [010] 10 ring of size 5.3 × 5.6 Å.

At high loadings, close to those of the most active Cu-ZSM-5 systems, cluster–cluster interactions will be present and therefore one must address the question of whether these interactions will influence the cluster configurations. In a previous study[14] we considered various Cu—OH—Cu clusters at infinite dilution (*i.e.* effectively eliminating any cluster–cluster interactions). The resulting configurations were consistent with those observed at high copper loading, which suggests that cluster–cluster interactions induce little perturbation of the cluster configuration and we suggest it is unlikely therefore that these interactions would prohibit or facilitate the formation of a particular structure.

Zeolite structure

The idealised structure of mordenite ($Na_8[Al_8Si_{40}O_{96}]\cdot 24H_2O$), illustrated in Fig. 1, is based on 5–1 secondary building units, linked into a series of chains and joined together to form two major channels. The space group symmetry is orthorhombic, *Cmcm* with unit cell $a=18.1$, $b=20.5$, $c=7.5$ Å and framework density 17.2T sites (1000 Å^3)$^{-1}$.[12] The mordenite structure has similarities to that of ZSM-5 (Fig. 1) which is also based on 5–1 secondary building units and comprises 17.9 T sites (1000 Å^3)$^{-1}$.

Potential models

Our approach is based on the use of static lattice methodologies, details of which are given elsewhere.[15,16] The methods have been extensively and successfully applied to model the structure and energetics of zeolite systems[17] and are based on the use of energy minimisation procedures which locate the low energy configurations of both framework and extra-framework atoms. Interatomic potentials are employed to describe the interactions between the component species of the system including long-range Coulombic terms, two- and three-body, parameterised short-range repulsive potentials; polarisability of the component species is introduced *via* the shell model.[18] The potential parameters for the zeolite were taken from Jackson and Catlow[19] while those for the copper from Sayle *et al.*[9] and, as previously, the calculations were performed using the Gulp code.[20] We emphasise that these procedures have been shown to reproduce accurately both framework structures and extra-framework cation positions for zeolitic systems.[17,19]

Generation of configurations for extra-framework copper species

For a unit cell of mordenite containing 96 T sites, the Si/Al ratio of 12 is achieved by replacing 8 silicon species by Al^{3+}. To accommodate a 150% exchange, four Cu^I and four Cu^{II} ions are introduced,[9] where 100% exchange represents $1Cu^+$ or $0.5Cu^{2+}$ per framework aluminium. The charge imbalance arising from the over-exchange is restored by introducing 4 OH^- species, which very probably corresponds to the behaviour of the real system. To model this system, trial structures were constructed by replacing, at random, eight of the 96 T sites with aluminium ions. The $4Cu^{II}$, $4Cu^I$, $4OH^-$ extraframework species are introduced into the zeolite, again randomly, with the only constraint imposed being a simple proximity criterion to prevent excessive steric overlap; potentially overlapping extra-framework species are rejected and a further random insertion applied. 2000 such trial structures were constructed, each with random aluminium distributions, and the energy of each system calculated. Final configurations were then obtained by applying a full energy minimisation to those 20 systems with the lowest energy. By considering only the most energetically favourable 20 systems, viable starting configurations are obtained. In a previous study, the ordering (by energy) of the 20 configurations initially generated, changed after full energy minimisation, accordingly in this study, the minimisation procedure initially adjusts the positions of the extra-lattice copper and hydroxy ions while maintaining a rigid lattice, after which, a full energy minimisation is performed, in which both the extra-framework and the host lattice species are allowed to relax. This procedure generates more reasonable starting configurations before commencing a full energy minimisation. As this initial minimisation step is computationally expensive, only 200 systems (instead of the 2000 considered previously) were considered and a full energy minimisation applied to the energetically most stable 20 systems, of which the ten lowest energy configurations are considered for analysis.

Results and Discussion

The configurations of the copper species in the ten systems with lowest energy are reported in Table 1(*a*)–(*j*) where (*a*) refers to the lowest energy system. In the final column of each table a cluster type (C1–C5) is indicated; a graphical representation of cluster configurations C1, C2 and C3 is given in Fig. 2.

Isolated copper species

Fig. 3 presents a histogram of the coordination number of isolated Cu^{II} species in mordenite together with comparable values for Cu^{II} species in ZSM-5.[21] No significant differences in the coordination numbers of the various isolated Cu^{II} species are observed between ZSM-5 or mordenite. However, the occurrence of $Cu^{II}-OH$ species is >50% more frequent in ZSM-5 than in mordenite.

Isolated Cu^I species with coordination numbers of two, three and four occur with similar frequencies within the ZSM-5 and mordenite host zeolites (Fig. 4). However, in contrast to ZSM-5, five-coordinate Cu^I species are not observed in mordenite suggesting that these species are energetically unfavourable with respect to alternative configurations in the structure. A study by Yamashita *et al.*[22] suggests that Cu^+ exists in mordenite with planar three-coordinate or linear two-coordinate geometry with slightly distorted symmetries.

We also note that only 35% of the total Cu^{II} ions exist either as isolated species or associated with OH, within the mordenite lattice, suggesting they are more stable as copper clusters, which compares with 53% for Cu^{II} species in ZSM-5 (30% of which are $Cu^{II}-OH$ species). Conversely Cu^I species are more likely to exist as isolated entities accounting for 60% of the total Cu^I introduced into the mordenite structure, compared with 65% for Cu^I in ZSM-5.

Copper association

Table 2 summarises the various configurations or cluster types and their frequency of occurrence for the copper species within the mordenite structure together with analogous results obtained in our previous study for Cu-ZSM-5; Fig. 5 shows the frequency of occurrence of cluster types C1–C5. The results suggest that mordenite entertains 11% more association of the copper species compared to ZSM-5 with 53% of the total copper species existing in clusters containing two, three or four copper ions. No copper clusters were observed which did not contain bridging hydroxy groups in accord with the Cu-ZSM-5 system. In addition clusters comprising two Cu^+ were not observed in accord with EXAFS data[22] on mordenite.

The model proposed previously for the active site in ZSM-5 comprises $Cu^{II}-OH-Cu^I$ species, designated C1 in Fig. 2. C1 clusters are also observed in Cu-mordenite although these account for only 10% of the total copper content compared with 25% in ZSM-5. In Cu-mordenite approximately equal occurrence of cluster types C1–C5 and isolated Cu^I species with three or four coordination are observed (Fig. 5) which suggests these species are of similar stability and are therefore expected to co-exist within the mordenite host. In contrast, the occurrence of C1 clusters in the ZSM-5 host lattice is significantly higher than alternative configurations and such clusters are expected to be the majority species within ZSM-5. We therefore suggest that the reduced activity for the Cu-mordenite compared with Cu-ZSM-5 may be attributed to the lower occurrence of $Cu^{II}-OH-Cu^I$ species.

A remarkable observation is that large clusters in Cu-mordenite, containing three or four copper species, account

Table 1 Bond distances, coordination number (CN) and association with framework aluminium (if applicable) for each of the copper ions within the ten systems considered[a]

	Cu—O/Å	Cu—OH/Å	Cu—Cu/Å	Cu—Al/Å	CN	structure
(*a*)						
$\mathrm{Cu^{II}}$	1.90, 1.98, 2.01, 2.29			2.87, 3.01	4	
	1.96, 2.03, 2.08, 2.15				**4**	
$\mathrm{Cu^{II}}$	1.95, 2.08	1.79		2.99	3	
	2.25, 2.29, 2.38	**1.78**			**4**	
$\mathrm{Cu^{II}}$	2.04, 2.23, 2.30, 2.31	1.72	3.27	3.03, 3.32	5	C1
	2.15, 2.22, 2.29, 2.31	**1.71**	**3.34**		**5**	
$\mathrm{Cu^{I}}$	1.98, 2.38	1.91		3.23	3	
	2.09, 2.20, 2.34	**1.93**			**4**	
$\mathrm{Cu^{II}}$	2.02, 2.25	1.71, 1.92	2.77	3.39	4	C3
	2.12, 2.13	**1.70, 1.87**	**2.69**		**4**	**C2**
$\mathrm{Cu^{I}}$	2.03, 2.09	1.89			3	
	2.08, 2.11	**1.92, 2.21**			**4**	
$\mathrm{Cu^{I}}$	2.00, 2.01			2.72	2	
	2.08, 2.14, 2.17				**3**	
$\mathrm{Cu^{I}}$	2.04, 2.11, 2.11, 2.19			2.77, 3.30	4	
	2.09, 2.11, 2.14				**3**	
(*b*)						
$\mathrm{Cu^{II}}$	1.91, 1.97, 2.31	1.78	3.30	2.88	4	C4
	2.13, 2.16, 2.16, 2.27	**1.76**	**3.28**		**5**	
$\mathrm{Cu^{II}}$	2.16, 2.21	1.70, 1.84	3.30, 3.24		4	
	2.06, 2.26	**1.71, 1.85**	**3.28, 3.26**		**4**	
$\mathrm{Cu^{I}}$	1.97, 2.00	1.93	3.24	2.73	3	
	2.05, 2.09	**1.92**	**3.26**		**3**	
$\mathrm{Cu^{II}}$	2.05	1.73, 1.80	3.14	3.01	3	C3
	2.14	**1.73, 1.77**	**3.26**		**3**	
$\mathrm{Cu^{I}}$	2.06, 2.23, 2.35	1.95		2.84	4	
	2.13, 2.15	**1.97**			**3**	
$\mathrm{Cu^{II}}$	1.89, 1.94, 2.04, 2.24			2.81, 3.34	4	
	2.02, 2.04, 2.09, 2.12				**4**	
$\mathrm{Cu^{I}}$	2.07, 2.08, 2.09, 2.13			2.74	4	
	2.01,2.06, 2.12, 2.20				**4**	
$\mathrm{Cu^{I}}$	1.98, 2.05, 2.16			2.81	3	
	2.05, 2.06, 2.23				**3**	
(*c*)						
$\mathrm{Cu^{II}}$	1.95, 1.95	1.70	3.45	2.98	3	C1
	1.98, 2.16	**1.69**	**3.41**		**3**	
$\mathrm{Cu^{I}}$	2.06, 2.25, 2.36	2.06		3.01	4	
	2.16, 2.22, 2.28	**2.02**			**4**	
$\mathrm{Cu^{II}}$	2.00, 2.01	1.81, 2.03	3.01	3.10	4	C2
	2.10, 2.15	**1.83, 1.91**	**3.30**		**4**	**C3**
$\mathrm{Cu^{II}}$	2.17, 2.21	1.80, 2.06			4	
	2.03, 2.08	**1.79**			**4**	
$\mathrm{Cu^{II}}$	1.93, 2.08	1.74		2.97	3	
	2.09, 2.37	**1.73**			**3**	
$\mathrm{Cu^{I}}$	1.92, 1.98, 2.11, 2.15			2.57	4	
	2.03, 2.03, 2.10, 2.23				**4**	
$\mathrm{Cu^{I}}$	2.01, 2.04, 2.05			2.79	3	
	2.00, 2.09, 2.14, 2.31				**3**	
$\mathrm{Cu^{I}}$	1.99, 2.00			2.70	2	
	2.03, 2.05				**2**	
(*d*)						
$\mathrm{Cu^{II}}$	1.96, 2.10	1.81, 1.85	2.93	2.97	4	C2
	2.20, 2.22	**1.80, 1.82**	**2.90**		**4**	
$\mathrm{Cu^{II}}$	1.99, 2.05	1.84, 1.88		2.95	4	
	2.11, 2.35	**1.83, 1.83**			**4**	
$\mathrm{Cu^{II}}$	1.89, 1.92, 1.97			2.85	3	
	1.95, 1.98, 2.09, 2.22				**4**	
$\mathrm{Cu^{II}}$	2.11	1.69, 1.76	3.34		3	C3
	2.26	**1.71, 1.80**	**3.26**		**3**	
$\mathrm{Cu^{I}}$	2.00, 2.07	1.95		2.81	3	
	2.06, 2.13	**1.91**			**3**	
$\mathrm{Cu^{I}}$	1.98, 2.02, 2.17			3.08	3	
	2.01, 2.07, 2.10				**3**	
$\mathrm{Cu^{I}}$	1.96, 2.03			2.77	2	
	2.07, 2.10				**2**	
$\mathrm{Cu^{I}}$	2.04, 2.07, 2.12			2.85	3	
	2.03, 2.12				**2**	
(*e*)						
$\mathrm{Cu^{II}}$	1.97, 2.03	1.83, 1.87	2.80	2.93	4	C2
	2.12, 2.13	**1.81, 1.84**	**2.79**		**4**	
$\mathrm{Cu^{II}}$	2.20, 2.26, 2.31	1.80, 1.82			5	
	2.13, 2.21	**1.80, 1.84**			**4**	
$\mathrm{Cu^{II}}$	1.98, 1.98, 2.08, 2.29			2.97	4	
	2.13, 2.14, 2.21, 2.23, 2.30				**5**	
$\mathrm{Cu^{II}}$	2.06, 2.13	1.74, 1.95	3.46	2.91	4	C3

Table 1 (*Continued*)

	Cu−O/Å	Cu−OH/Å	Cu−Cu/Å	Cu−Al/Å	CN	structure
	2.16	**1.72, 1.83**	**3.43**		**3**	
Cu^{I}	2.16, 2.22	1.91			3	
	2.20, 2.25, 2.28	**1.92**			**4**	
Cu^{I}	1.99, 2.00, 2.17, 2.21			2.78	4	
	2.12, 2.15, 2.15, 2.16				**4**	
Cu^{I}	2.00, 2.03, 2.32			2.79	3	
	2.08, 2.09, 2.13				**3**	
Cu^{I}	2.00, 2.14, 2.16, 2.24			2.93	4	
	2.11, 2.14, 2.19, 2.20				**4**	
(*f*)						
Cu^{II}	1.87, 1.93, 2.09, 2.10			2.80	4	
	2.00, 2.03, 2.04, 2.19				**4**	
Cu^{II}	1.88, 1.97	1.70	3.24	2.85	3	C1
	2.32, 2.33, 2.36	**1.68,**	**3.26**		**4**	
Cu^{I}	2.07, 2.32	1.92		3.21	3	
	2.10, 2.19	**1.91**			**3**	
Cu^{II}	1.91, 2.21	1.86, 1.92	3.00	3.00	4	C2
	2.16, 2.24	**1.84, 1.94**	**2.96**		**4**	
Cu^{II}	1.98, 2.30	1.83, 1.95			4	
	2.05, 2.16	**1.83, 1.92**			**4**	
Cu^{I}	2.02, 2.02, 2.24			2.70	3	
	2.06, 2.10, 2.15				**3**	
Cu^{I}	1.96. 2.02, 2.14			2.79	3	
	2.01, 2.18, 2.18				**3**	
Cu^{I}	1.97, 2.11	2.00		3.34	3	
	2.03, 2.06	**1.95**			**3**	
(*g*)						
Cu^{II}	2.05, 2.23	1.78	3.43	3.33	3	C4
	2.07	**1.80, 1.82**	**3.37**		**3**	
Cu^{II}	2.14	1,70, 1.78	3.43, 3.30		3	
	2.09	**1.71, 1.82**	**3.37, 3.37**		**3**	
Cu^{I}	2.01, 2.04	1.91	3.30	2.79	3	
	2.08, 2.14	**1.90**	**3.37**		**3**	
Cu^{II}	1.91, 1.98, 1.99	1.82		2.92, 3.00	4	
	2.05, 2.10, 2.30	**1.76**			**4**	
Cu^{II}	1.90, 1.97, 2.05, 2.19			2.79	4	
	1.92, 2.00, 2.24				**3**	
Cu^{I}	2.08, 2.10, 2.19, 2.22			2.86	4	
	2.09, 2.20, 2.22, 2.29				**4**	
Cu^{II}	2.04, 2.12, 2.19, 2.31			3.25	4	
	2.04, 2.08, 2.11, 2.18				**4**	
Cu^{I}	2.02, 2.07, 2.12, 2.29			2.69	4	
	2.04, 2.13, 2.19, 2.25				**4**	
(*h*)						
Cu^{II}	1.82, 1.85			2.82	2	
	1.90, 1.97				**2**	
Cu^{II}	1.92, 1.93	1.78	3.43	2.89	3	C5
	2.05, 2.19, 2.21	**1.76**	**3.41**		**4**	
Cu^{II}	2.12	1.77, 1.86, 1.89	3.43, 2.67, 3.26	3.31	4	
	2.34	**1.81, 1.84, 1.88**	**3.41, 2.76, 3.46**		**4**	
Cu^{I}	2.15, 2.21, 2.25	2.05, 2.10	2.67, 3.12	2.88	5	
	2.18, 2.34	**2.00, 2.03**	**2.76, 2.79**		**4**	
Cu^{I}	2.10, 2.11, 2.27	1.94	3.26, 3.12	2.90	4	
	2.05, 2.20	**1.96**	**3.46, 2.79**		**3**	
Cu^{II}	2.08, 2.11, 2.24	1.78		3.01	3	
	2.02	**1.73**			**2**	
Cu^{I}	1.96, 2.01, 2.07, 2.23			2.76	4	
	2.12, 2.18, 2.19, 2.21				**4**	
Cu^{I}	2.00, 2.12, 2.17, 2.23			3.13, 3.22	4	
	1.98, 2.08, 2.12, 2.30				**4**	
(*i*)						
Cu^{II}	1.88, 1.91, 1.95			2.86	3	
	1.99, 1.99, 2.09, 2.22				**4**	
Cu^{II}	2.03, 2.07, 2.24	1.69	3.34	2.88	4	C5
	2.13, 2.15, 2.22	**1.68**	**3.36**		**4**	
Cu^{I}	2.06, 2.32	1.96, 1.99	2.34, 3.58		4	
	2.09	**1.96, 1.98**	**3.36, 3.53**		**3**	
Cu^{II}	2.21	1.71, 1.73	3.50, 3.58		3	
	2.10	**1.72, 1.73**	**3.46, 3.53**		**3**	
Cu^{I}	2.06, 2.14	1.93	3.50		3	
	2.05, 2.09	**1.92**	**3.46**		**3**	
Cu^{II}	2.08, 2.18, 2.26	1.71	3.43	3.00	4	C1
	2.07, 2.22, 2.23, 2.25	**1.68**	**3.12**		**5**	
Cu^{I}	2.04, 2.14	1.97		2.74	3	
	2.00, 2.12	**1.89**			**3**	
Cu^{I}	2.08, 2.11, 2.27			2.71, 3.02	3	
	2.15, 2.18, 2.21, 2.31				**4**	

Table 1 (*Continued*)

	Cu—O/Å	Cu—OH/Å	Cu—Cu/Å	Cu—Al/Å	CN	structure
(*j*)						
Cu^I	2.02, 2.21	1.92	2.95	2.75	3	C5
	2.09, 2.19	**1.93**	**3.19**		**3**	
Cu^{II}	2.11, 2.18	1.72, 1.84	3.45, 2.95	3.00	4	
	2.22	**1.71, 1.81**	**3.45, 3.20**		**3**	
Cu^{II}	2.14	1.72, 1.81	3.45, 3.30		3	
	2.19, 2.28	**1.73, 1.84**	**3.45, 3.36**		**4**	
Cu^I	1.99, 2.05	1.94	3.30	2.76	3	
	2.04, 2.14	**1.93**	**3.36**		**3**	
Cu^{II}	1.99, 2.07	1.79			3	
	2.02, 2.03	**1.80**			**3**	
Cu^{II}	1.98, 2.08, 2.16			3.04	3	
	2.04, 2.11, 2.12				**3**	
Cu^I	2.05, 2.19, 2.22			2.77	3	
	2.07, 2.12, 2.21, 2.21				**4**	
Cu^I	2.00, 2.08, 2.25			2.81	3	
	2.04, 2.14				**2**	

[a] In this table (*a*) is the most energetically favourable system and (*j*) the least. The number in the final column refers to a cluster type (illustrated in Fig. 2) which best illustrates the configuration of the particular copper cluster. The numbers in bold refer to the analogous systems where all the aluminium species have been replaced by silicon. Thus, the lowest energy system, (*a*), contains two copper pairs, cluster types C1 and C3 and four isolated copper species. The C1 cluster comprises of a Cu^{II} ion with a coordination number of five and a Cu^I species with CN = 3 with a copper–copper separation of 3.27 Å.

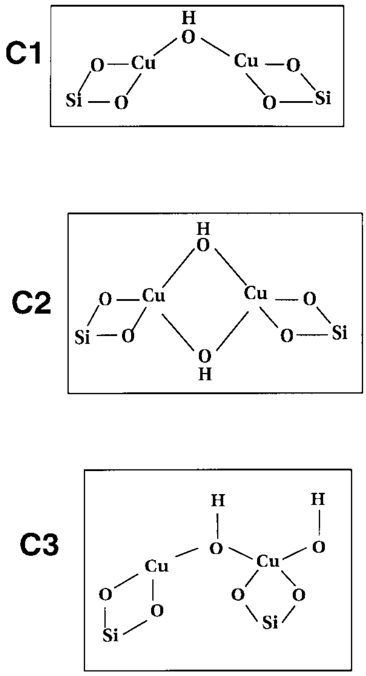

Fig. 2 Diagrammatic representations of the cluster types C1–C3. C4 and C5 clusters are not shown as they do not conform to a 'general' structure (see Fig. 6), suffice to say they represent clusters containing three and four copper species respectively.

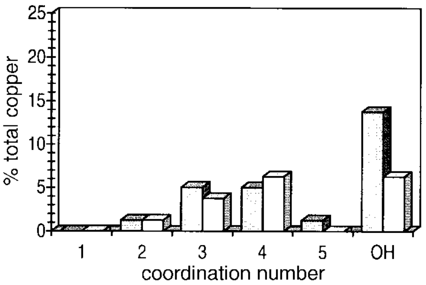

Fig. 3 Relative proportions of isolated Cu^{II} species in mordenite (unshaded) as a function of coordination number. OH represents Cu^{II}—OH species. Values for Cu^{II} in ZSM-5 (shaded) are given as a comparison.

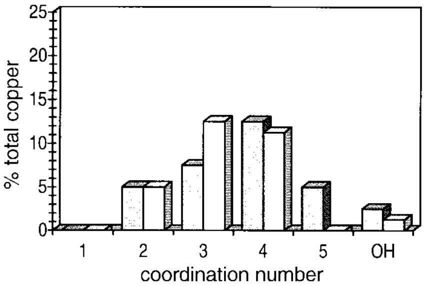

Fig. 4 Relative proportions of isolated Cu^I species in mordenite (unshaded) as a function of coordination number. OH represents Cu^I—OH species. Values for Cu^I in ZSM-5 (shaded) are given as a comparison.

for 22% of the total copper content. One such cluster, comprising [Cu^{II}—OH—Cu^I—OH—Cu^{II}—OH—Cu^I], lies along the wall of the zeolite and is illustrated in Fig. 6. If such large clusters are likely models for the active site one might also expect to see a high proportion of these clusters in Cu-ZSM-5, since this system exhibits significantly higher catalytic activity for NO decomposition compared with Cu-mordenite. However, only one cluster, comprising three copper species, was observed in the analogous Cu-ZSM-5 study and we suggest that such clusters are unlikely to feature in the catalysis.

The identification of a high proportion of complex clusters comprising three or four copper species and three hydroxy groups within Cu-mordenite increases confidence in the search procedure for identifying all low energy configurations. In addition, this finding reinforces our previous argument that these species are not observed in ZSM-5 as they are unstable with respect to alternative configurations rather than being attributable to an inadequate search procedure.

Copper coordination

The saturation of the coordination of the copper species is expected to influence the catalytic activity and therefore it is useful to compare the coordination of the copper species in mordenite and ZSM-5. Table 3 gives the average coordination numbers for copper species in the mordenite host lattice calculated over the six lowest energy systems together with

Table 2 A summary of the various configurations or cluster types and their occurrence for the copper species within the mordenite lattice together with analogous results obtained in our previous study for Cu-ZSM-5. Values are given as a percentage of the total number of copper species introduced over all the ten systems

	ZSM-5 (%)	mordenite (%)
isolated copper species		
2-coord.	6.25	6.25
3-coord.	12.5	16.25
4-coord.	17.5	17.5
5-coord.	6.25	0
Cu—OH	16.25	7.5
total	58.75	47.5
copper clusters		
Cu_2	0	0
$Cu_2(OH)$	25	10
$Cu_2(OH)_2$	12.5	20
$Cu_3(OH)_n$	3.75	7.5
$Cu_4(OH)_n$	0	15
total	41.25	52.5

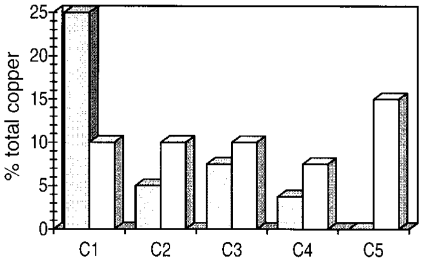

Fig. 5 Relative proportions of the cluster types C1–C5 in Cu-mordenite (unshaded) and Cu-ZSM-5 (shaded)

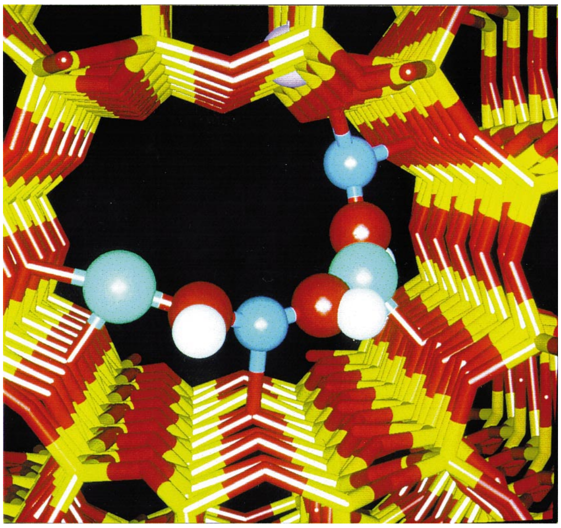

Fig. 6 Representation of the [$2Cu^{II}$,$2Cu^{I}$,3OH] cluster, observed in Table 1(*i*). Framework oxygen and silicon species are represented by the red and yellow sticks respectively, extra-lattice hydroxy groups are the red and white spheres and extra-lattice Cu^{II} and Cu^{I} are the small and large blue spheres respectively.

analogous values for Cu-ZSM-5. The coordination number is 0.21 higher for the Cu^{II} species and 0.21 lower for Cu^{I} species in mordenite compared with ZSM-5, and, although this factor may indeed influence the catalytic activity, it is unlikely to rationalise the order of magnitude difference in activity between the two systems.[13]

Role of framework aluminium

In a previous study of Cu-ZSM-5 we identified a strong association between framework aluminium species and the extra-framework copper.[10] This association resulted in both significant structural modifications of the copper clusters and large changes in the coordination number of these copper species.[11] Furthermore, as these structural changes are likely to influence the catalytic properties, these observations may help rationalise the relationship between the Si/Al ratio, copper loading and the catalytic activity of the material.[23] To this end, each of the ten lowest energy systems were again energy minimised after replacing all of the aluminium with silicon atoms. Charge neutrality was maintained by distributing the excess charge equally over all the silicon atoms. The configurations (bond distances and coordination numbers) of the copper species after all the aluminiums have been replaced with silicon are reported in bold type in Table 1(*a*)–(*j*).

The large changes (Table 3) in coordination number for Cu^{II} (+0.46) and Cu^{I} (−0.12) in the purely siliceous form of the zeolite, silicalite, compared to the aluminosilicate form, ZSM-5, are not reproduced in mordenite where the average coordination number of the copper species remain constant. However, the framework aluminium remains central to the configuration of the copper clusters: the presence of framework aluminium anchors the copper ions, in particular Cu^{II}, to the zeolite wall in accord with Cu-ZSM-5, as can be seen from Table 3, the average Cu^{II}—O bond distance in Cu-mordenite is 0.1 Å lower for the aluminosilicate compared with the purely siliceous form. In addition, in Table 1(*a*), when the framework aluminium species are replaced by silicon, the C3 copper pair [Cu^{II}—$(OH)_2$—Cu^{I}] changes to a C2 cluster [Cu^{II}—OH—Cu^{I}—OH] and in Table 1(*c*) the C2 cluster changes to a C3 cluster when the adjacent aluminium species is replaced by silicon. Such configurational changes show once more that framework aluminium exacts a critical influence on the structure of these copper clusters.

Conclusion

In this study we have identified significant differences between the configurations of copper species in the ZSM-5 and mordenite host lattices. Moreover, such differences in the structures of the copper-containing clusters are strongly dependent on the local environment imposed by the host lattice, particularly with respect to framework aluminium species. These differences may help provide a structural explanation of the much reduced activity of Cu-mordenite compared with Cu-ZSM-5: in particular, the occurrence of Cu^{II}—OH—Cu^{I} species, which previously

Table 3 Average coordination numbers and Cu—O bond distances for Cu^{I} and Cu^{II} species in mordenite over the six lowest energy systems (*a*)–(*f*). Values for ZSM-5 calculated in a previous study are given as a comparison. The numbers in bold refer to bond distances and coordination numbers in the purely siliceous form of the zeolites.

	ZSM-5	MOR
	coordination number	
Cu^{II}	3.42	3.63
	3.88	**3.68**
Cu^{I}	3.54	3.33
	3.42	**3.33**
	bond distances/Å	
Cu^{II}—OH	1.76	1.80
	1.79	**1.80**
Cu^{I}—OH	1.96	1.94
	1.96	**1.97**
Cu^{II}—O	2.05	2.06
	2.14	**2.16**
Cu^{I}—O	2.10	2.09
	2.13	**2.12**

we suggested represent a useful model for the active site in Cu-ZSM-5, is much lower in mordenite. The results provide further support for the crucial role of such clusters in effecting the NO decomposition catalysis.

D.C.S would like to thank R.P. for financial support. We are grateful to MSI for the provision of the InsightII software used to construct the images in this work.

References

1 M. Iwamoto, S. Yokoo, S. Saskai and S. Kagawa, *J. Chem. Soc., Faraday Trans. 1*, 1981, **77**, 1629.
2 R. Burch, *Catal. Today* 1995, **26**, 97 and references therein.
3 M. Iwamoto, H. Yahiro, N. Mizuno, W.-X. Zhang, Y. Mine, H. Furukawa and S. Kagawa, *J. Phys. Chem.*, 1992, **96**, 9360.
4 W. Grunert, N. W. Hayes, R. W. Joyner, E. F. Shpiro, M. R. Rafiq, H. Siddiqui and G. N. Baeva, *J. Phys. Chem.*, 1994, **98**, 10832.
5 E. S. Shpiro, R. W. Joyner, W. Grunert, N. W. Hayes, M. Rafiq, H. Siddiqui and G. N. Baeva., *Stud. Surf. Sci. Catal.*, 1994, **84**, 1483.
6 R. J. Blint, *J. Phys. Chem.*, 1996, **100**, 19 518
7 W. F. Schneider, K. C. Hass, R. Ramprasad and J. B. Adams, *J. Phys. Chem.*, 1996, **100**, 6032.
8 T. J. Truex, R. A. Searles and D. C. Sun, *Platinum Met. Rev.*, 1992, **36**, 2.
9 D. C. Sayle, C. R. A. Catlow, J. D. Gale, M.-A. Perrin and P. Nortier. *J. Phys. Chem. A*, 1997, **101**, 3331.
10 D. C. Sayle, C. R. A. Catlow, M.-A. Perrin and P. Nortier, *J. Chem. Soc., Chem. Commun.*, 1995, 945.
11 D. C. Sayle, C. R. A. Catlow, M.-A. Perrin and P. Nortier, *J. Mater. Chem.*, 1997, **7**(8), 1635.
12 W. M. Meier and D. H. Olson, *Atlas of Zeolite Structure Types*, Butterworths, Cambridge University Press, UK, 1987, and references cited therein.
13 Y. Li and K. Hall, *J. Catal.*, 1991, **129**, 202.
14 D. C. Sayle, C. R. A. Catlow, M.-A. Perrin and P. Nortier, in preparation.
15 *Computer Simulation of Solids, Lecture notes in Physics 166*, ed. C. R. A. Catlow and W. C. Mackrodt, Springer, Berlin, 1982.
16 C. R. A. Catlow, D. H. Gay, L. Ackermann, R. G. Bell, S. Holt, D. M. Lewis, M. A. Nygren, G. Sastra, D. C. Sayle and P. E. Sinclair, *J. Mol. Catal. A: Chem.*, 1997, **115**, 431.
17 *Modelling of Structure and Reactivity in Zeolites*, ed. C. R. A. Catlow, Academic Press, London, 1992.
18 B. G. Dick and A. W. Overhauser, *Phys. Rev.*, 1958, **112**, 90.
19 R. A. Jackson and C. R. A. Catlow, *Mol. Simul.*, 1988, **1**, 207.
20 J. D. Gale, *J. Chem. Soc., Faraday Trans.*, 1997, **93**, 629.
21 R. A. Schoonheydt, *Catal. Rev. -Sci. Eng.*, 1993, **35**, 129.
22 H. Yamashita, M. Matsuoka, K. Tsuji, Y. Shioya, M. Anpo and M. Che., *J. Phys. Chem.*, 1996, **100**, 397.
23 G. Moretti, *Catal. Lett.*, 1994, **28**, 143.

Paper 7/02840G; *Received* 25*th April*, 1997